Session 51

Remote sensing of coral reefs: transitioning from developmental to operational

Session chairs:

Eric J. Hochberg, eric.hochberg@bios.edu

Stuart Phinn, s.phinn@uq.edu.au

Chris Roelfsema, c.roelfsema@uq.edu.au

Collin A, Laporte J, Koetz B, Martin-Lauzer F-R, Desnos Y-L (2016) Mapping bathymetry, habitat, and potential bleaching of coral reefs using Sentinel-2. Proceedings of the 13th International Coral Reef Symposium, Honolulu: 373-387

Mapping bathymetry, habitat, and potential bleaching of coral reefs using Sentinel-2

Antoine Collin, Jean Laporte, Benjamin Koetz, François-Régis Martin-Lauzer, Yves-Louis Desnos

Abstract Global ocean warming combined with a long-lasting El Niño Southern Oscillation event (2015–-2016) are provoking the third ever global coral bleaching event. Hotspots of marine biodiversity, coral reefs require special attention from stakeholders and scientists tasked with Earth's health. Earth observation has recently benefited from the launch of the multispectral Sentinel-2 (S2) sensor delivering high spatial resolution (10 m) optical information worldwide every 10 days. Within the Sen2Coral project of ESA, and as a precursor of open-source specific data processors' development, this study strives to evaluate in real conditions the S2 capabilities for coral reef bathymetry and habitat mapping as well as bleaching detection given the ongoing event. A dedicated campaign held in Fatu Huku (Marquesas Archipelago, French Polynesia) in February 2016 enabled geolocated water depths and benthic frames to be extensively collected. After geometric and radiometric standardization, two sets of S2 blue, green, red and near-infrared bands were processed for comparison (11 February and 11 April 2016). The bathymetry mapping up to 20 m was satisfactorily generated for both dates (R^2=0.64, r=0.79, RMSE=0.12 and R^2=0.74, r=0.86, RMSE=0.09, respectively). The benthic composition (deep water, sand, reef pavement and live reef) was also reasonably classified (OA=78.8%, κ=0.71 and OA=73.5%, κ=0.65). Bathymetric maps and difference maps of benthic composition and depth-invariant reflectance were used to evaluate changes in water surface, water column and benthic habitats of this oceanic lagoon. By focusing on areas deprived of water-related constraints, benthic shifts from live reef to reef pavement were locally pointed out suggesting a potential bleaching detection at this 10-m scale when fit in the radiometric error budget. Those findings hold great promise to use S2 for coral reef bathymetry and habitat mapping but also are an incentive to confirm bleaching detection over larger areas provided with denser ground-truth data, unequivocally correlating the bleaching event over S2 data.

Key words: bathymetry, habitat, mapping, bleaching, high resolution, Sentinel-2 Satellite

Antoine Collin
Ecole Pratique des Hautes Etudes, UMR Prodig, 15 boulevard de la mer, 35800 Dinard, France

Antoine Collin
Laboratoire d'Excellence CORAIL, France

Jean Laporte, François-Régis Martin-Lauzer
ARGANS Ltd, 1 Davy Road, Plymouth Science Park, Plymouth PL6 8BX, United Kingdom

Benjamin Koetz, Yves-Louis Desnos
ESA-ESRIN, Via Galileo Galilei, Casella Postale 64, 00044 Frascati, Italy

Communicating author: Antoine Collin antoine.collin@ephe.sorbonne.fr

Introduction

Shallow tropical coral reefs host more than a quarter of the marine biodiversity and provide crucial ecosystem goods and services such as food production, climate change regulation, and amenities (The Economics of Ecosystems and Biodiversity 2010). In the Anthropocene era, multi-scale spatial pressures have however caused the 19% loss and 75% endangering of worldwide coral reefs (Wilkinson 2008; Burke et al. 2011). The raising awareness of coral reefs risks in the scientific and public communities have prioritized the monitoring of coral reef socio-ecosystems' dynamics in response to current hazards, exposure and vulnerability.

Even though coral reefs concentrate biodiversity at significant rates, their monitoring based on handborne surveys cannot be achieved given the very low surface-time ratio and the cost associated with remote, isolated areas. Likewise, waterborne observation is not possible over very shallow reef ecosystems. Spaceborne coral reef remote sensing has become a toolbox to gain insights into benthic structure (Collin and Hench 2012), composition (Roelfsema et al. 2013) and health indicators (Collin and Planes 2012; Rowlands et al. 2012). As a massive, pathologic event, coral bleaching has been investigated by multispectral satellite sensors, such as the 30-m Landsat TM (Yamano and Tamura 2004) and 4-m IKONOS (Elvidge et al. 2004). A pioneer study investigated the potential of the 10-m Sentinel-2 (S2) sensor, launched by the European Space Agency (ESA), to map tropical shallow coral reefs, including bleaching (Hedley et al. 2012). The narrowness of the optical

spectral bands and the enhanced spatial resolution have improved the discrimination of benthic composition. Moreover, high revisit rate, worldwide coverage and open access data make S2 a robust asset to build time-series of coral reef health. However, this paper was based on simulated image analyses. Even if the inherent uncertainty of models was quantified, a real-world study is still needed.

Since 2014, severe bleaching events occurred in the North and South Pacific Ocean, as well as the Indian Ocean and Caribbean Sea (Eakin et al. 2016). Bleaching is caused by the expulsion of zooxanthellae symbiotic algae comprised into coral tissues in response to stressing water temperature anomalies. The ongoing (2015–2016) El Niño Southern Oscillation continues the bleaching in Pacific and Indian Oceans and is very likely to resume in the Caribbean for a second consecutive year.

In this study, we turned the current bleaching challenge into an opportunity to evaluate the capabilities of S2 to detect the coral reef bleaching and to map bathymetry and benthic composition in real conditions. A campaign was primarily organized to survey coral reefs of Fatu Huku Island (Fig. 1) in the Marquesas Archipelago (French Polynesia), given the high susceptibility of bleaching (equatorial central Pacific Ocean), the lack of local disturbances (uninhabited and very low fishery pressure), and the challenge in a rough place where in situ monitoring is problematic.

Materials and methods

Study site and ground-truth campaign

The study site is located in the presque-lagoon of Fatu Huku Island (9°26’10’’S, 138°55’26’’W). Contrary to other Marquesas Islands, Fatu Huku shows a tangible coral reef structure at the seascape level, including channel, barrier reef and outer reef (Fig. 1). As uninhabited, this island is not threatened by local anthropogenic activities but is thereafter very few studied. Spanning 1.3 km², the central island is topped by a plateau of an over-raised atoll with a maximum elevation of 361 m. The island receives a low range of precipitation (800-1,000 mm per year), what strongly alleviates the sedimentation stress.

A ground-truth campaign was carried out to collect geolocated spectral and acoustic data from the benthos on 22-24 February 2016 across predetermined transects (red lines in

Fig. 1). An array of 208’ high resolution underwater video data (GoPro Hero 3 1920 × 1080 with 24 frames per second) and 74,724 echosounder data points (Lowrance HDS 7 Gen3 200

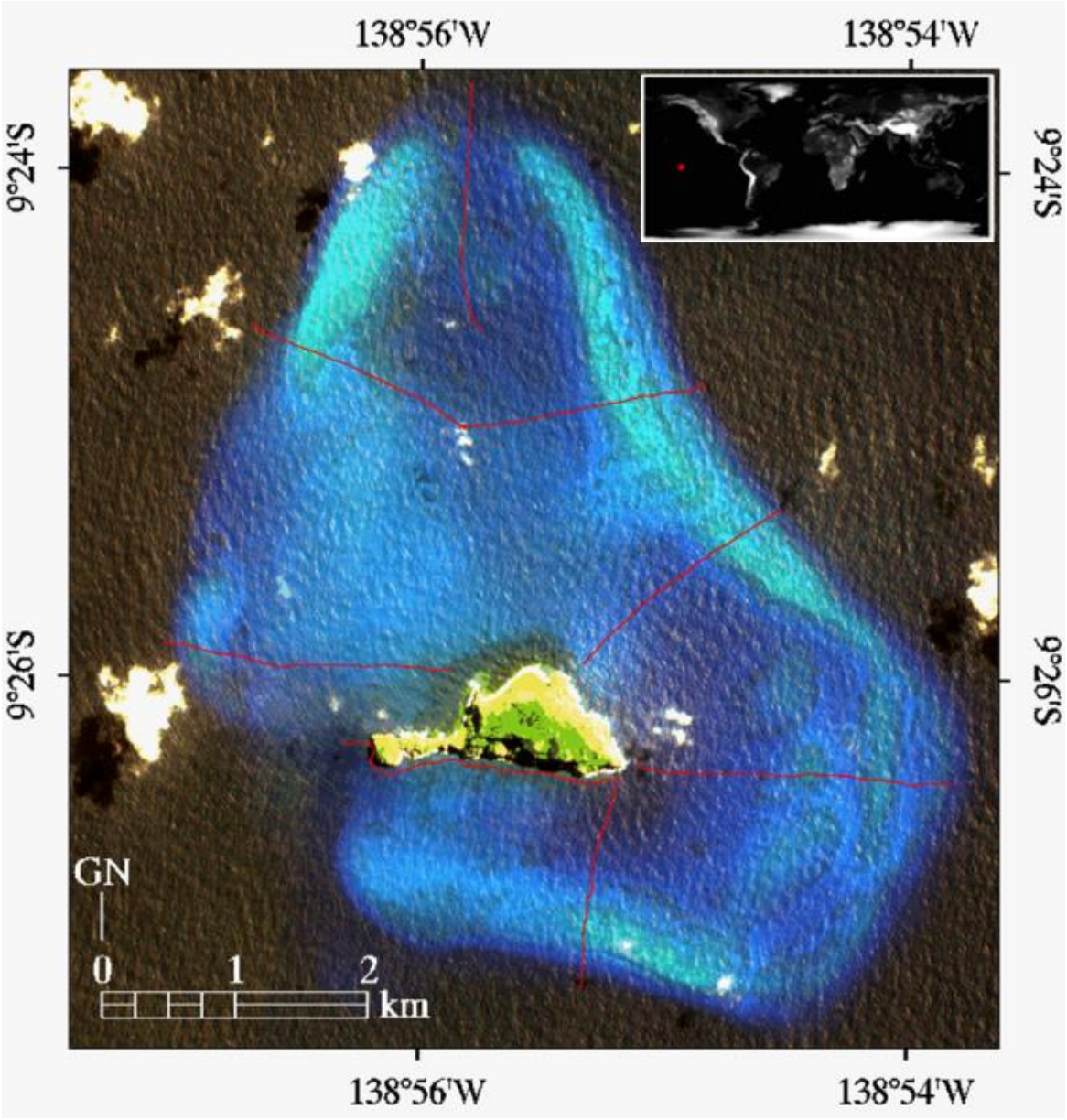

Fig. 1 Natural coloured image (Red: 4th S2 band, Green: 3rd S2 band, Blue: 2nd S2 band) of the study site (Fatu Huku, Archipelago of the Marquesas Islands, French Polynesia). The sampling transects are showed in red lines

kHz) were collected alongside with accurate GNSS locations (Lowrance HDS 7 Gen3 10 Hz) from a fine-tuned structure mounted on a small boat (Fig. 2).

Spaceborne imagery

S2 data were collected every 10 days, courtesy of the ESA S2 program manager, to be analysed in a time series with available and soon-to-be-developped data processors. Out of

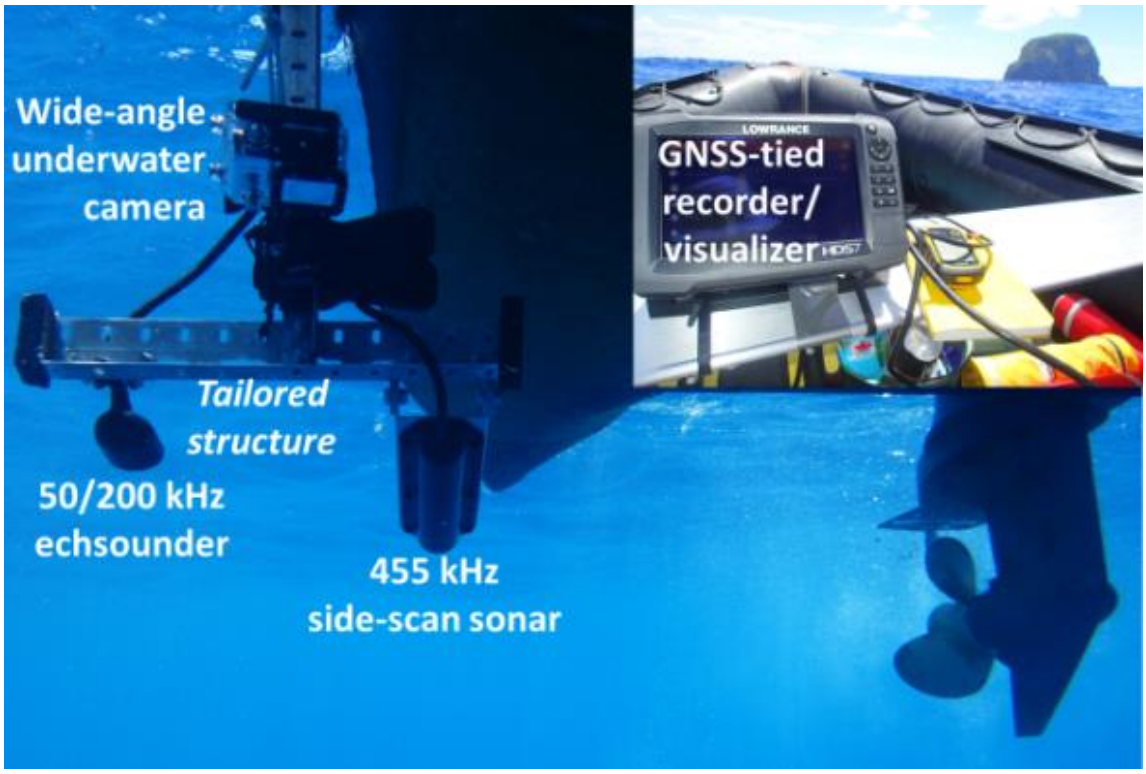

Fig. 2 Waterborne instrumentation composed of a GNSS/SoNAR combo device (data recorder/visualizer provided with GNSS linked with echosounder and side-scan SoNAR) and a wide-angle underwater camera mounted on a shallow structure

the S2 multispectral datasets of February to May, two were selected on 11 February and 11 April 2016 over Fatu Huku as tasked by ESA in the Sen2Coral Project. Launched in 2015, S2 leverages 13 spectral bands from the visible to infrared gamut with pixel size ranging from 10 to 60 m. The four investigated bands match the highest pixel size (Table 1).

Preliminary geometric and radiometric corrections were applied to the four-band imagery by using, as a first step, the dedicated S2 module in the geospatial software ENVI (Harris Geospatial, Boulder, CO, USA), i.e. conversion of 12-bit Digital Number (DN) into at-sensor radiance (W m^{-2} st^{-1} μm^{-1}), then application of MODerate resolution TRANsmittance-cored Fast Line-of-site Atmospheric Analysis of Spectral Hypercubes

package correcting for atmospheric attenuation and adjacency effects, thus providing water-leaving reflectance (unitless as reflectance = radiance-irradiance ratio).

Table 1 Spectral specificities of the four 10-m Sentinel-2 bands investigated for coral reef mapping

Band number	Central wavelength	Bandwidth
2	490	65
3	560	35
4	665	30
8	842	115

Preliminary geometric and radiometric corrections were applied to the four-band imagery by using, as a first step, the dedicated S2 module in the geospatial software ENVI (Harris Geospatial, Boulder, CO, USA), i.e. conversion of 12-bit Digital Number (DN) into at-sensor radiance (W m^{-2} st^{-1} μm^{-1}), then application of MODerate resolution TRANsmittance-cored Fast Line-of-site Atmospheric Analysis of Spectral Hypercubes package correcting for atmospheric attenuation and adjacency effects, thus providing water-leaving reflectance (unitless as reflectance = radiance-irradiance ratio).

Imagery pre-processing

Prior to correcting for hydrologic attenuation, required for the benthic purposes, two additional procedures have been applied. Given the focus on underwater features, masks were built and applied onto the terrestrial area but also onto the clouds and inherent shadows (Fig. 3A and 3B). Since Fatu Huku is an open ocean island, significant swell contributes to sun glint over S2 imagery. A sun deglinting procedure was therefore applied so that the three visible bands could be corrected for specular reflection. The standardized method relied on the regression of the visible bands against the infrared reflectance over deep water (no benthic reflectance) areas (Hedley et al. 2005) (Fig. 3C and 3D):

$$R'_i = R_i - s_i(R_{NIR} - min_{NIR}) \quad (1)$$

where R'_i is the deglinted reflectance band i, R_i the glinted reflectance band i, s_i the slope of the regression between R_i and R_{NIR} reflectance bands. Since reflectance is exponentially attenuated by the water column height (i.e., bathymetry), the water-leaving reflectance is required to be duly corrected to obtain benthic reflectance:

$$R'_{ib} = (R'_i - R'_{i\infty})e^{2kz} + R'_{i\infty} \quad (2)$$

where R'_{ib} is the benthic deglinted reflectance band i, $R'_{i\infty}$ is the benthic deglinted reflectance band i over deep water, k is the diffuse attenuation coefficient, and z is the water depth. Since Fatu Huku lagoon did not benefit from fine-scale hydrographic charts, the absence of knowledge in z hindered the computation of R'_{ib}. Circumventing difficulties in *a priori* parameterizing z and k in (2), the procedure of the depth-invariant indices was selected (Watkins 2015). This hydrospheric correction is based on the calculation of the ratio of diffuse attenuation coefficients for deglinted reflectance bands:

$$Depth - invariant\ index_{ij} = ln(R'_i) - \left(\left(\frac{k_i}{k_j}\right) \times \ln(R'_j)\right) \quad (3)$$

where:

$$\left(\frac{k_i}{k_j}\right) = a + \sqrt{(a^2 + 1)} \quad (4)$$

where:

$$a = \frac{\sigma_i - \sigma_j}{2\sigma_{ij}} \quad (5)$$

with σ_i and σ_j the variances of the deglinted reflectance bands i and j, and σ_{ij} the covariance between deglinted reflectance bands i and j over sand sites at various water depths (blue squares on Fig. 3E and 3F). The computation of the ratios of diffuse attenuation coefficients is indicated in Table 2. Resulting three depth-invariant indices (i.e. blue-green; blue-red and green-red) may be integrated in the form of a RGB composite image (Fig. 3E and 3F).

Bathymetry and benthic mapping

As a robust proxy for understanding the coral reef ecology, the bathymetry was mapped based on S2 visible bands by applying a reflectance band ratio transformation (Stumpf et al.

2003) and calibrating the obtained ratio with soundings pruned at 20 m depth. This method relies on the differentiation of optical light attenuation by water in respect to waveband: longer wavebands are, more attenuated they are. The bathymetry was solved as follows:

$$z = m_1 \frac{\ln(nR_i)}{\ln(nR_j)} - m_0 \quad (6)$$

where m_1 and m_0 are the slope and intercept of the best calibration model and n is constant to ensure the positivity of natural logarithm. A digital depth model was generated with a 10 m × 10 m pixel size.

The classification of the benthic composition was achieved using ground-truth video frames associated with S2 pixels. Out of 104' across 4 exploitable transects, 354 frames were retrieved as a rate of one frame every 30'' and utilized to classify transect pixels into 4

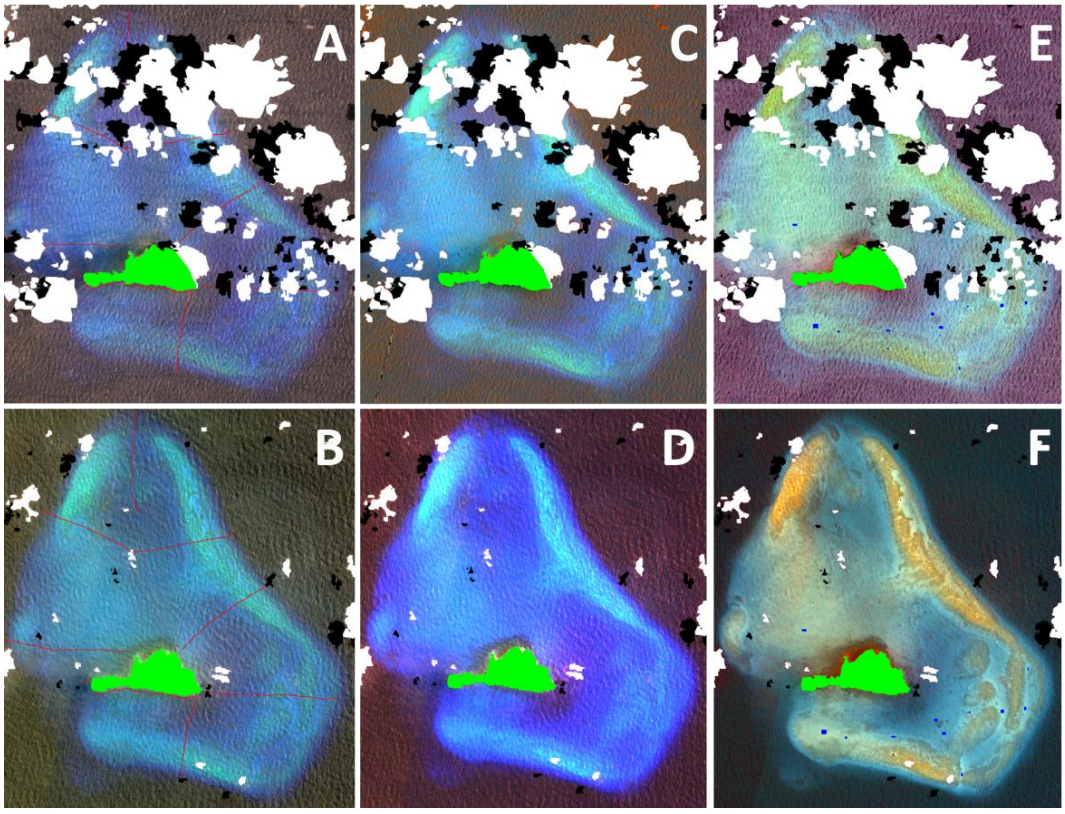

Fig. 3 Preliminary procedures applied to both dated Sentinel-2 imageries in order to (A and B) mask out land, clouds and tied shadows, (C and D) remove the specular reflection, and (E and F) correct for hydrospheric attenuation by computing depth-invariant indices (blue rectangles correspond to sand benthos at various water depths)

Table 2 Three ratios of diffuse attenuation coefficients based on pairs of deglinted reflectance bands

Date	Blue-Green	Blue-Red	Green-Red
11 Feb. 2016	0.72	0.75	0.04
11 Apr. 2016	1.01	0.21	2.77

benthic classes: deep water, sand, reef pavement and live reef pixels. Each class was randomly subdivided into a training and a validation dataset composed of 67 and 33 pixels, respectively. Training pixels were implemented as input data to aid the maximum likelihood algorithm establish specific depth-invariant deglinted reflectance signatures for each class and then assign remaining pixels to the most likely class. Validation pixels were used to build a confusion matrix leading to the quantification of the classification process accuracy, based on overall accuracy (OA) and kappa coefficient (κ) (Congalton and Green 2008).

Coral bleaching detection

In the context of the third-ever global bleaching event, an attempt to detect this potential event in Fatu Huku was performed. Change detections were examined using both initial (11 February 2016) and final (11 April 2016) depth-invariant indices and supervised classifications. Changes in depth-invariant indices were reckoned by normalizing data ranges (between 0 and 1) and classifying into 11 change classes to check the magnitude of change. Regarding habitat classification, change maps for every class was produced alongside with inherent statistics.

Results

The bathymetry mapping extracted from S2 imageries was satisfactorily computed across Fatu Huku lagoonal depth ranges but also over time (Fig. 4). Despite a substantial cloud/shadow coverage, actual water depths were well modelled by an exponential model

fitting 11 February S2 data (R^2=0.64, r=0.79 and RMSE=0.12 m, Fig. 4A and 4B). Shallower areas (in blue) topped at 8 m on the barrier reef whilst deeper ones (in burgundy) bottomed at 20 m in the channel. Benefiting from a very low cloud/shadow coverage, 11 April S2 bathymetry retrieval was carried out almost completely on the lagoon with a very good agreement (R^2=0.74, r=0.86, RMSE=0.09 m, Fig. 4C and 4D). An increase in variance around the fitted model occurred at 14 m.

The benthic habitat mapping derived from S2 datasets processed at the depth-invariant deglinted reflectance level provided reasonable results for both dates: OA=78.8% and 73.5%; κ=0.71 and 0.65 for 11 February (Fig. 5A) and 11 April (Fig. 5B), respectively. Underlying confusion matrices indicated that only 36% and 40% of live reef validation pixels were correctly classified for 11 February and 11 April, whereas the majority of deep water, sand and reef pavement validation pixels were well classified (100%/94%, 79%/73%, 100%/88%,

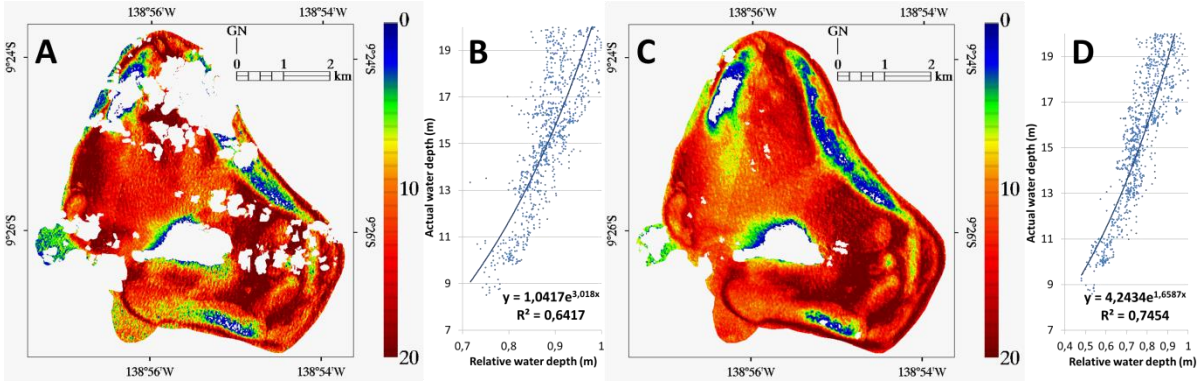

Fig. 4 Bathymetric maps retrieved from visible Sentinel-2 reflectance bands and associated calibrating functions based on hydrographic soundings for 11 February 2016 (A and B, respectively) and 11 April 2016 (C and D, respectively)

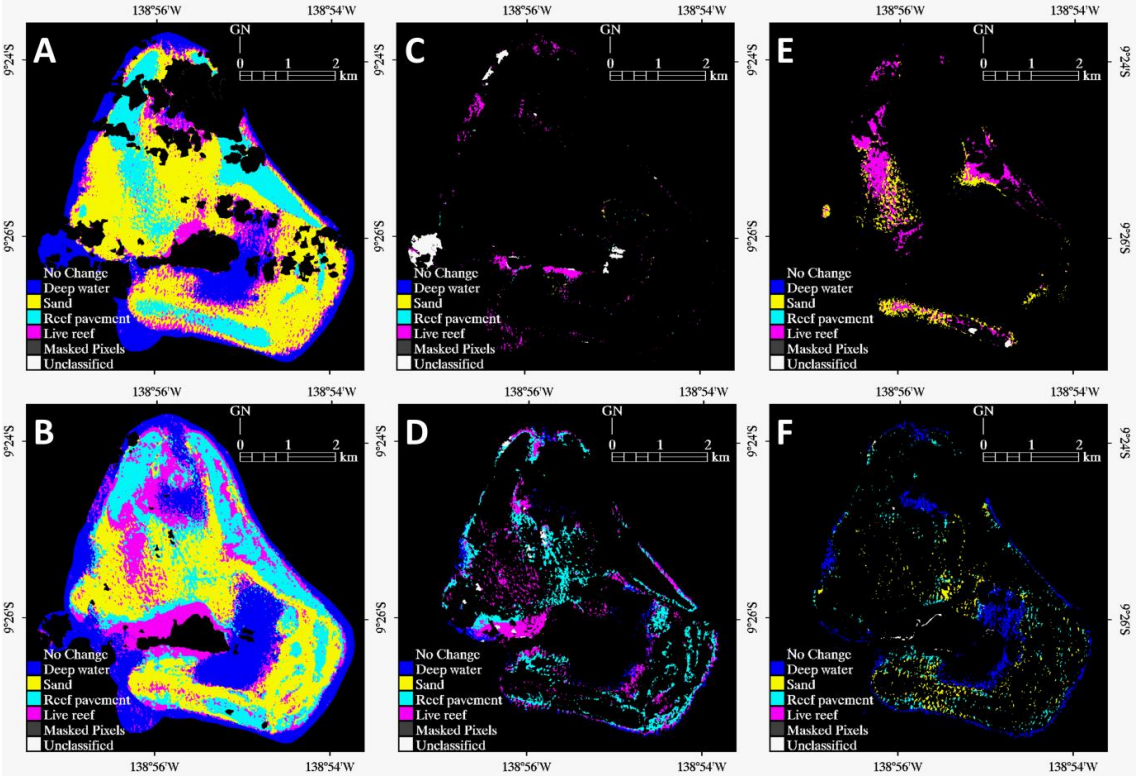

Fig. 5 Classification maps resulted from depth-invariant deglinted reflectance Sentinel-2 bands for (A) 11 February 2016, (B) 11 April 2016 and their difference focusing on (C) deep water, (D) sand, (E) reef pavement and (F) live reef classes

respective of dates). Difference maps of the four benthic classes indicated substitution of: initial deep water pixels southward island by final live reef ones (N=3,869, Fig. 5C), initial sand northwestward island by final live reef and initial sand southward lagoon by final reef pavement (N=14,198 and N=18,540, Fig. 5D), initial reef pavement southward northwestern barrier reef by final live reef (N=10,981, Fig. 5E), and initial live reef eastward island by final deep water and erratic reef pavement (N=10,174 and N=4,309, Fig. 5F).

Changes in depth-invariant indices between 11 February and 11 April 2016 were overall consistent across Fatu Huku lagoon for blue-green and blue-red indices: predominance of negatives changes (blue in Fig. 6A and 6B) around the terrestrial and boundary areas and absence of changes (gray in Fig. 6A and 6B) more located in the southern part of the lagoon. Regarding the green-red index, negatives changes also occurred around the terrestrial island and circumference of the lagoon but positive changes took place over reef areas (pavement or live) all around the lagoon (as shown in red in Fig. 6C).

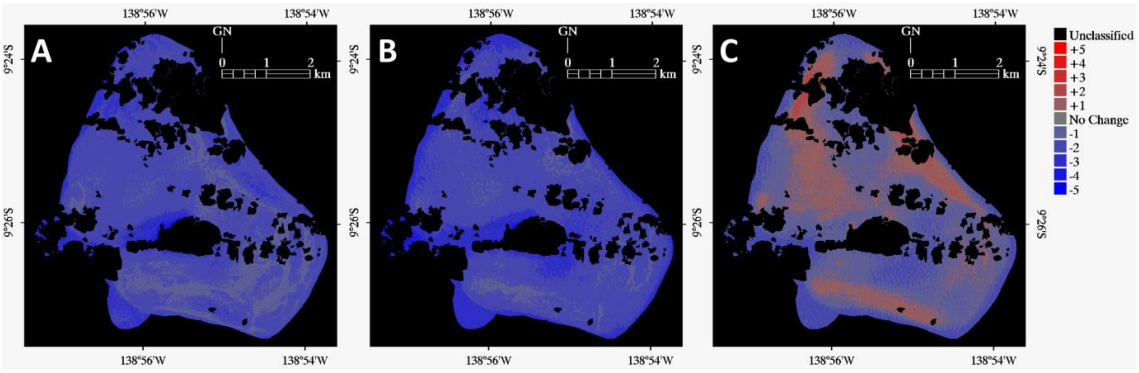

Fig. 6 Difference maps between (A) blue-green, (B) blue-red and (C) green-red depth-invariant indices based on the initial 11 February 2016 and final 11 April 2016 visible deglinted reflectance Sentinel-2 datasets

Discussion

The evaluation of S2 capabilities for coral reef mapping was characterized by good performances regarding both bathymetry and benthic composition. An in-depth analysis of the biplot between sonar and S2-modelled water depth data revealed that data up to 14 m could be neatly extracted (RMSE=0.07 m) by S2 information calibrated by accurate soundings. Even though the agreement between actual and modelled depth data was higher for the acquisition deprived of clouds/shadows, the overall consistency in retrieval over time promotes the S2 sensor as a robust tool for studying coral reef structural complexity. It is noteworthy that these findings lacked from very shallow reef features (shallowest reefs topped only at 8.5 m in Fatu Huku) so as to quantify the accuracy of S2-mediated bathymetry in the 0-10 m range, flagship for the biodiversity but also vulnerability. On the other hand the difference in two dates' bathymetry occurred toward the south of the northwestern barrier reef and south of the island in the form of "virtual" shallower and deeper bottoms, respectively (see Fig. 4A and 4B). This difference is likely not to stem from a shift in the benthic structure but rather either from distinct inherent optical properties (IOP's) of the water column or from the roughness of the water surface. The first assumption is supported by massive bodies of suspended solids we experienced northward island during February campaign as attested by video frames. This oceanic island is indeed very subject to easterly trades, which re-suspend and transport solids. Further work should investigate the S2 capabilities to derive the IOP's of various water turbidity classes. The surface roughness

entailed an increase in specular reflection but also anisotropic transmission, which may result in a decrease of reflectance along the visible gamut.

The spatial distribution of benthic habitats was conveniently rendered according to the training and validation datasets, making S2 sensor a serious competitor of Landsat-8 to map coral reef benthos. However it is important to bear in mind that poorest classification scores took place with live reef (susceptible for bleaching) for both dates. This finding corroborates studies (Hochberg et al. 2003, Leiper et al. 2009) demonstrating that complex spectral signatures across visible wavelengths tied to both "brown" and "purple" coral reefs are considerably better discriminated by hyper- or superspectral sensors than standard multispectral ones (provided with the three natural colours). The examination of the evolution of the class substitution between both dates identified the change of deep water (south of the island) and reef pavement (south of the northwestern barrier reef) into live reef and sand, respectively. Both changes could be correlated with an initial surface roughness (as shown by specular patterns of the bathymetry, Fig. 4A) driving a diminution of the benthic reflectance to "darker" habitats (Hochberg et al. 2003). The class substitution over time also featured a shift of sand (northwestward island) and reef pavement (southward northwestern barrier reef) into live reef but also a shift of live reef (eastward island) into deep water. The juxtaposition of the bathymetry outcome (highlighting a plume-like pattern, Fig. 4B) might explain changes into "darker" benthos by the increase in water column turbidity composed of sediment or phytoplankton (Maritorena et al. 1994).

Following the previous findings linking bathymetry and benthic composition (initial southern specular reflection and final northern turbidity), it is more judicious to focus on changes prevailing over areas deprived of surface roughness or solid re-suspension, namely the easternmost spit. Two benthic habitat changes predominated: the shift of sand to reef pavement (Fig. 5D) and the shift of live reef to reef pavement (Fig. 5F). These changes geographically corresponded to a slight decline in both blue-green and blue-red depth-invariant indices (Fig. 6A and 6B). Coral spectroscopy concords with such results insofar as sand, unhealthy or bleached hard corals display a lower blue/green and blue/red reflectance ratios compared to healthy corals (Hochberg et al. 2003, Yamano and Tamura 2004, Leiper et al. 2009). Even though these preliminary attempts to detect coral bleaching using S2 in the real world are promising, it is duly advocated to confirm such capabilities by focusing on

shallower and larger areas provided with denser ground-truth time-series to accurately link the bleaching event with S2 data. In parallel, another group of the ESA-funded team from ARGANS-ACRI has studied radiometric changes within an error budget model, using bespoke tools that will be insightfully implemented over high temporal S2 data such as the 3 months EO acquisition of Fata Huku from February to May.

Acknowledgements

First author gratefully acknowledges the European Space Agency and Argans-Acri for funding and organizing this work, including the scientific campaign. Material support for the field measurements came from the Ecole Pratique des Hautes Etudes. Catamaran ITEMATA staff is acutely thanked for navigation and field support.

References

Burke L, Reytar K, Spalding M, Perry A (2011) Reefs at risk revisited. World Resources Institute, Washington, DC

Collin A, Hench JL (2012) Towards deeper measurements of tropical reefscape structure using the WorldView-2 spaceborne sensor. Remote Sensing 4: 1425-1447

Collin A, Planes S (2012) Enhancing coral health detection using spectral diversity indices from worldview-2 imagery and machine learners. Remote Sensing 4: 3244-3264

Congalton RG, Green K (2008) Assessing the accuracy of remotely sensed data: principles and practices. CRC press

Elvidge CD, Dietz JB, Berkelmans R, Andrefouet S, Skirving W, Strong AE, Tuttle BT (2004) Satellite observation of Keppel Islands (Great Barrier Reef) 2002 coral bleaching using IKONOS data. Coral Reefs 23: 123-132

Hedley J, Roelfsema C, Koetz B, Phinn S (2012) Capability of the Sentinel 2 mission for tropical coral reef mapping and coral bleaching detection. Remote Sensing of Environment 120: 145-155

Hochberg EJ, Atkinson MJ, Andréfouët S (2003) Spectral reflectance of coral reef bottom-types worldwide and implications for coral reef remote sensing. Remote Sensing of Environment 85: 159-173

Kumar P (2010) The Economics of Ecosystems and Biodiversity: ecological and economic foundations. UNEP/Earthprint

Leiper IA, Siebeck UE, Marshall NJ, Phinn SR (2009) Coral health monitoring: linking coral colour and remote sensing techniques. Canadian Journal of Remote Sensing 35: 276-286

Maritorena S, Morel A, Gentili B (1994) Diffuse Reflectance of Oceanic Shallow Waters: Influence of Water Depth and Bottom Albedo. Limnol and Oceanogr 39: 1689-1703

Roelfsema C, Phinn S, Jupiter S, Comley J, Albert S (2013). Mapping coral reefs at reef to reef-system scales, 10s–1000s km2, using object-based image analysis. International journal of remote sensing, 34: 6367-6388

Rowlands G, Purkis S, Riegl B, Metsamaa L, Bruckner A, Renaud P (2012) Satellite imaging coral reef resilience at regional scale. A case-study from Saudi Arabia. Marine Pollution Bulletin 64: 1222-1237

Stumpf RP, Holderied K, Sinclair M (2003) Determination of water depth with high-resolution satellite imagery over variable bottom types. Limnol and Oceanogr 48:547-556

The Economics of Ecosystems and Biodiversity (2010) The economics of ecosystems and biodiversity ecological and economic foundations. Pushpam Kumar (ed) Earthscan, London and Washington

Watkins RL (2015) A Methodology for classification of benthic features using WorldView-2 Imagery. NOAA contract number WE-133F-15-SE-0518, 29 pp

Wilkinson C (2008) Status of Coral Reefs of the World. Global Coral Reef Monitoring Network and Reef and Rainforest Research Center, Townsville, Australia. 296 pp

Yamano H, Tamura M (2004) Detection limits of coral reef bleaching by satellite remote sensing: simulation and data analysis. Remote Sensing of Environment 90: 86-103